Solute inaccessible aqueous volume changes during opening of the potassium channel of the squid giant axon

Joshua Zimmerberg,*‡ Francisco Bezanilla,‡§ and V. Adrian Parsegian*‡

*Unit on Molecular Forces and Assembly, Laboratory of Biochemistry and Metabolism, National Institute of Diabetes and Digestive and Kidney Diseases, and the Physical Sciences Laboratory, Division of Computer Research and Technology, National Institutes of Health, Bethesda, Maryland 20892; ‡Marine Biological Laboratory, Woods Hole, Massachusetts 02543; and §Department of Physiology, Ahmanson Laboratory of Neurobiology and Jerry Lewis Neuromuscular Research Center, University of California, Los Angeles, California, 90024

ABSTRACT We have applied solutions with varying osmotic pressures symmetrically to the inside and outside of perfused, TTX-treated, giant axons. The potassium conductance G decreased with increasing osmotic stress, but there was no effect on either the shape or the position of the voltage-current curve. One must distinguish three possible actions of the osmotic agent: osmotic stress, channel blocking, and lowered solution conductivity. To do so, we compared results obtained working with pairs of internal and external solutions of either (*a*) equal osmotic stress, (*b*) equal conductivity, or (*c*) the same blocking agent. There was the same change in G irrespective of the type of stressing species (sorbitol or sucrose); this provides some evidence against a blocking mechanism. The conductivity of the *external* solution had a small effect on K currents; internal solution conductivity had none. A change in series resistance of the Schwann cell layer could account for the small effect of external solution conductivity. The primary cause of G depression appears, then, to be the applied osmotic stress. Using this result, we have developed models in which the channel has a transition between closed states under voltage control but osmotically insensitive and a closed/open step that is voltage-independent but osmotically sensitive. We have assumed that the conductance of this open state does not change with osmotic stress. In this way, we estimate that an additional 1,350 ± 200 Å^3 or 40–50 molecules of solute-inaccessible water appear to associate with the average delayed rectifier potassium channel of the squid axon when it opens.

INTRODUCTION

By their very nature, selective channels exclude all but those few molecular species which they are specifically designed to conduct. Substances that are excluded might attempt to enter the pore, to bind near the pore entrance, or to congregate to "block" and impede the passage of acceptable species. But excluded species must also act osmotically on the channel interior. A high enough osmotic pressure from excluded species can, in principle, exert an osmotic stress to collapse the aqueous volume from which they are excluded. If a channel exhibits states of different conductance, then it is likely that these different states will possess different amounts of internal water. If the space occupied by the internal water is inaccessible to excluded solutes, then it is entirely possible that the application of osmotic stress through impermeant species should change the probabilities of occupation of the different states.

By exploiting this change in energy of channel conductance states, it was possible to infer the internal aqueous volume changes in reconstituted "mitochondrial porin" or "voltage-dependent anion channels" (VDAC) as they opened and closed in a single step driven by applied voltage (Zimmerberg and Parsegian, 1986). This paper describes our experience applying osmotic stress to make a similar measurement on delayed rectifier potassium (K) channels in perfused squid axons.

Kinetic analysis of potassium channels, combined with ionic and pharmacologic manipulation of the media bathing the channels, has led to several models that describe their time- and voltage-dependent conductance in excitable tissues (Hodgkin and Huxley, 1952*a*, *b*, *d*; Cole and Moore, 1961; Young and Moore, 1981; Gilly and Armstrong, 1982; White and Bezanilla, 1985). These channels inactivate slowly compared to the time of measurements (Hodgkin et al., 1952*c*; Ehrenstein and Gilbert, 1966). It is possible to perfuse both sides of the membrane containing the channel while recording the macroscopic conductances that indicate the open-to-closed equilibrium of many channels (Baker et al., 1962; Bezanilla et al., 1982).

In the following, we describe the axonal response to solutions containing added sucrose or sorbitol. We interpret the suppression of K conductance in hyperosmotic solutions as due to the action of osmotic stress and predict the amount of solute-inaccessible water that associates with the opening K channel.

METHODS AND MATERIALS

Theoretical

Earlier papers describe the use of osmotic stress, the tension that develops within a solute-inaccessible space in

equilibrium with a solution having an osmotic pressure (Π_{osm}) of that solute species, to measure intermolecular forces (Parsegian et al., 1986) or the internal aqueous volume changes of opening channels (Zimmerberg and Parsegian, 1986). We define the change in mean pore volume (Δv) as the volume of water that must enter a solute-inaccessible part of the channel when it opens. The corresponding osmotic work of opening is the product of Π_{osm} and Δv, ($\Pi_{osm} \cdot \Delta v$). It is due to the osmotic pressure of all species unable to enter the open K^+ channel. It is as if the small channel opening acted as a semipermeable membrane on either mouth of the channel. To be thermodynamically well defined, this osmotic pressure must be the same on both sides of the membrane. The ratio of open to closed channel probabilities for an opening step C $\leftrightarrow$ O then depends on the osmotic energy as

$$(\text{Open})/(\text{Closed}) = (\text{O})/(\text{C}) \propto e^{-(\Pi_{osm} \cdot \Delta v/kT)}, \qquad (1)$$

where k is the Boltzmann constant and T temperature in degrees Kelvin.

There exist many models for gating states. We find it possible to capture the essential features of gating and opening under osmotic stress with either parallel or serial schemes. For the serial CC_nO model, gating and opening involve stepping through completely closed voltage-dependent states followed by an osmotically sensitive, voltage-insensitive opening step:

$$C_0 \underset{K_\psi(\Psi)}{\longleftrightarrow} C_n \underset{K_\pi(\Pi_{osm})}{\longleftrightarrow} O.$$

The fraction of open channels is

$$\frac{K_\pi}{1 + K_\pi + (1/K_\psi)}.$$

When conductance measurements used for estimation of Δv are taken at fully saturating voltages $K_\psi >> 1$.

The measured potassium conductance G is the sum of conductances of N independently opening channels. If the channels can only be fully closed or fully open with a single channel conductance g, then for $K_\psi >> 1$,

$$G = Ng \frac{(\text{O})}{(\text{O}) + (\text{C}_n)}. \qquad (2)$$

We write the equilibrium constant K_π for the opening step in the form $A \exp[-(\Pi_{osm} \cdot \Delta v/kT)]$ where A is assumed to be voltage independent. The ratio of two macroscopic conductances measured at two different osmotic stresses, Π_1 and Π_2, is a function of Δv:

$$\frac{G_2}{G_1} = \frac{\exp(-\Pi_2 \cdot \Delta v/kT)}{\exp(-\Pi_1 \cdot \Delta v/kT)} \cdot \frac{1 + A \exp(-\Pi_1 \cdot \Delta v/kT)}{1 + A \exp(-\Pi_2 \cdot \Delta v/kT)}. \qquad (3)$$

Given the empirical G_1, G_2, Π_1, and Π_2, and an estimate for the nonosmotic factor A, one may compute Δv. The detailed procedure for making this computation is given in the Appendices. In the limit where $\Delta\Pi \cdot \Delta v \geq kT$ and $(\text{O})/(\text{C}) << 1$, this last equation takes on the simple form,

$$\ln(G_2/G_1) = -\frac{\Pi_2 - \Pi_1}{kT} \cdot \Delta v. \qquad (4)$$

Eq. 3 provides an operational definition of Δv for the sequential model described here and in the Appendices.

In the parallel model the voltage-sensitive gating and the osmotically sensitive conformational change are independent, and behave as a series of two separate barriers to channel ion flux. In this case Eq. 4 yields Δv, but without requiring limits $\Delta\Pi \cdot \Delta v \geq kT$ and $(\text{O})/(\text{C}_n) << 1$.

Once the propriety of such models is demonstrated, the principal obstacle to the use of this equation is the worry that the solutes one adds (to change Π_{osm}) might also be modifying nonosmotic factors. The apparent macroscopic conductance may, for example, decrease from channel blockage or from lowered conductivity of the bathing solution. (One may think of the latter as an altered series resistance either around the axon membrane or at the single channel level.)

The usual way to identify Π_{osm} as the operative variable has been to verify that one obtains the same effect from applying chemically different species at the same osmotic strength (Parsegian et al., 1986; Zimmerberg and Parsegian, 1986; Zimmerberg and Whitaker, 1985; Rau et al., 1984; Parsegian, 1983). In the present study, we not only use different osmotic agents, but also recognize that these different agents will change solution conductivity to different extents. We check to see whether we can explain our results by invoking changes in series resistance.

Experimental

Giant axons were dissected from squid (*Loligo pealei*) and the axoplasm removed. Axons were cleaned, cannulated, perfused, and voltage-clamped in the traditional way (Bezanilla et al., 1982). Temperature was held at 10°C with a Peltier device and negative feedback control. The basic internal solution was 160 mM K glutamate, 40 mM KF, 10 mM Tris-HCl, pH 7.2, to 0.98 Osm/kg with sucrose; external solution 480 mM Tris, 10 mM KCl, 10 mM $CaCl_2$, 50 mM $MgCl_2$, pH 7.6. Hyperosmotic solutions were produced by adding dry nonelectrolyte (sucrose or sorbitol) to prepared ionic solutions. In this way ionic activities should be unchanged in all solutions. This was verified for calcium and potassium activity by testing with ion-specific electrodes. Hypoosmotic solutions were made by lowering the sucrose concentration in the internal solution and lowering the Tris concentration to 400 mM in the external; control isoosmotic solutions for hypoosmotic experiments were made by adding sucrose to

both hypoosmotic solutions. The isoosmotic solutions for the conductivity control experiments were: for internal, 160 mM K glutamate, 40 mM KF, 10 mM Tris-HCl, pH 7.2, to 0.98 Osm/kg with sucrose or sorbitol; for external, 140 mM Tris-HCl, 10 mM $CaCl_2$, 50 mM $MgCl_2$, pH 7.6, to 0.98 Osm/kg with Tris, sucrose, or sorbitol. Osmotic pressures were measured with a vapor pressure osmometer (Wescor Inc., Salt Lake City, UT) for solutions whose osmotic pressure is < 3.8 Osm/kg. The higher osmotic pressures of two of the sorbitol solutions were estimated by measuring the molarity of four sorbitol solutions equilibrated with vapors of four different saturated salts with known vapor pressures, and assumed additivity with the salts of the isoosmotic. Conductivities were measured with an AC bridge meter (Yellow Springs Instrument Co., Yellow Springs, OH). All external solutions contained 300 nM tetrodotoxin. Chemicals were from Sigma Chemical Co. (St. Louis, MO).

Command voltage pulses were provided by a computer/digital interface (Stimers et al., 1987). Axons were held at a −70-mV holding potential, and stepped to various voltages in a modification (P/−2) of the P/4 protocol (Bezanilla and Armstrong, 1977). The depolarizing potential was usually held for a fixed duration for each axon, and was followed by either a 20-mV decrement in voltage, or a return to the holding potential. Next the membrane was stepped to −100 mV (subtracting holding potential), and the same test pulses were applied twice at half the amplitude and in the opposite direction. The net current is the sum of the test pulse plus the two subtracting pulses. Conductance was determined by two methods. In the first, the instantaneous change in current at the end of the depolarizing pulse was divided by the pulse voltage (Gilly and Armstrong, 1982). In the second, instantaneous conductances were measured by dividing the change in current during the −20-mV perturbation by 20 mV. Electrode junction potentials were measured for all test solutions with the same chamber and electrodes, and did not change with osmotic stress.

RESULTS

Hyperosmotic stress

An example of the change in current as a function of time is shown in Fig. 1 *a*. Tetrodotoxin-treated axons were held at −70 mV, the membrane potential was then stepped to various voltages, and then returned to −70 mV. The currents are predominantly K currents; leakage current has been subtracted out (Stimers et al., 1987). Large tail currents are seen as first reported by Frankenhaeuser and Hodgkin (1956) and interpreted by them as evidence for the large accumulation of K ions in the Schwann cell layer. The K current response was depressed when both

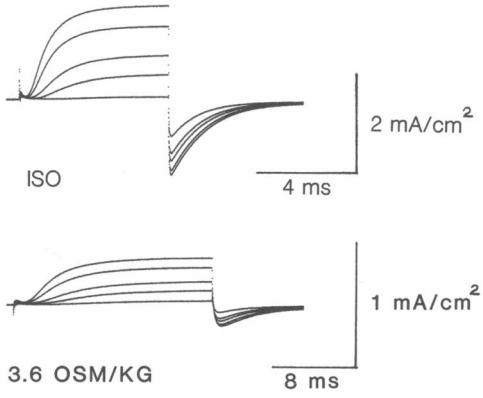

FIGURE 1 Current vs. time after a step in voltage. Note the suppression of current after application of osmotic stress (through perfusion of hyperosmotic sucrose solutions). Note also the slowed response. The voltage here is pulsed from −70 mV to the test voltage, then back to −70 mV.

internal and external solutions were made hyperosmotic with sucrose (Fig. 1 *b*). This treatment also slowed the response, and accumulation of potassium was decreased. A small rounding of the exponentially decaying tail

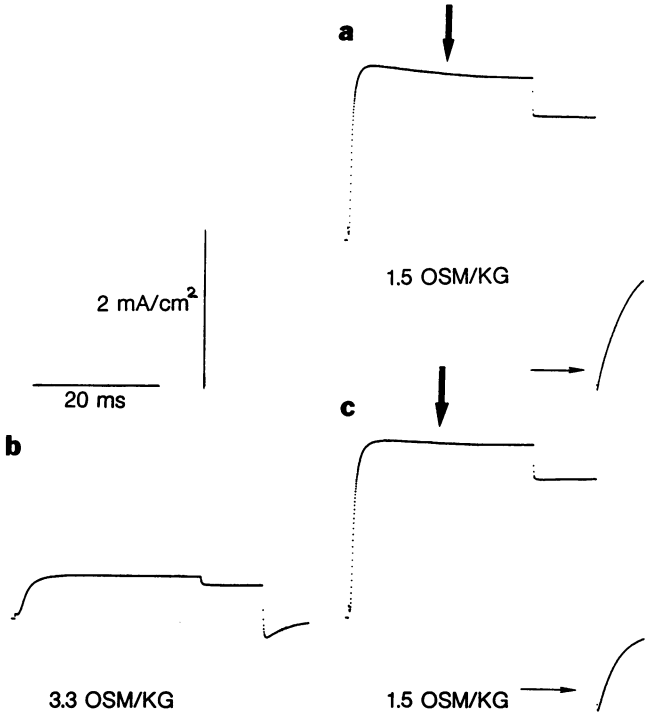

FIGURE 2 Voltage is pulsed from −70 to +80 mV, then to +60 mV, then back to −70 mV in solutions of, successively, (*a*) 1.5 Osm/kg, (*b*) 3.3 Osm/kg, and (*c*) again 1.5 Osm/kg. Accumulation (decay and tail current amplitude, arrows) seems permanently to be lost after exposure to osmotic stress.

currents was seen upon returning the axon to the resting potential.

We could not return axons to normal isoosmotic solutions without substantially increasing current leakage. But we found we could test for reversibility of the effect of osmotic stress by being able to return axons from a hyperosmotic solution to a less hyperosmotic solution. The K current traces in Fig. 2 illustrate long (20 ms) pulses applied to an axon that was subjected to 1.5, 3.3, then again 1.5 Osm/kg sucrose solutions. Initially, there is evidence of some decrease in the i_K later in the pulse—a phenomenon usually associated with the accumulation of exiting potassium ions in the Schwann cell layer (Frankenhaeuser and Hodgkin, 1956; Taylor et al., 1980). At 3.3 Osm/kg, currents are reduced. On return to lower osmolality, the potassium conductance recovered and accumulation was reduced.

The steady-state G vs. Ψ (Fig. 3) shows a decrease in conductance measured at two osmotic pressures, 1.9 Osm/kg and 3.3 Osm/kg. The 3.3 Osm/kg data, rescaled to the isoosmotic data, show no shift in the $G - \Psi$ curve (Fig. 2). Here, and below in Figs. 4 and 5, data from each axon at different osmotic pressures were rescaled to examine voltage dependence by superimposing points at limiting conductance.

Axons subject to successive hyperosmotic solutions showed reversible changes in G as a function of solution Π_{osm} (Fig. 5; note the order of solutions.) Often there was a slow steady deterioration of the axonal currents over periods of hours. But at no time was there a change in the shape of the voltage dependence or of the voltage at half-maximal conductance (Ψ_0). Rescaled data from partially stressed (1.4 Osm/kg) axons were superimposed upon data from those under full hyperosmotic stress (3.6 Osm/kg) (Fig. 4).

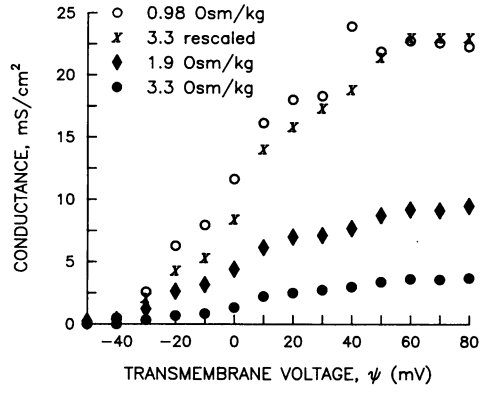

FIGURE 3 Steady state K conductance vs. voltage in normal (0.98 Osm/kg) and two hyperosmotic (1.9, 3.3 Osm/kg) sucrose solutions. Osmotic stress does not seem to affect the voltage dependence of the conductance. (Compare the normal curve O and the 3.3 Osm/kg data X rescaled to coincide at high voltage.) Voltage here is pulsed from −70 mV to the test voltage.

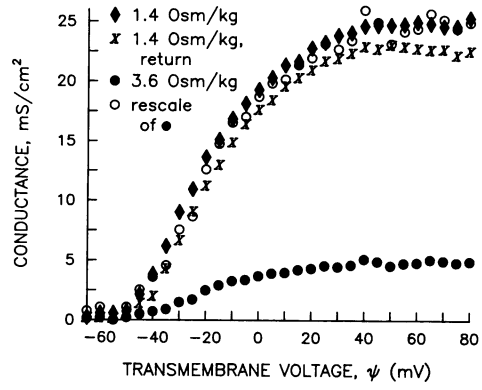

FIGURE 4 Potassium conductance G vs. applied voltage for squid giant axon. The voltage was stepped from −70 mV holding potential to the indicated voltage and held for 8 mS. An "instantaneous" conductance was taken from the change in current when the voltage was subsequently dropped by 20 mV. Axons were initially perfused with 160 mM K glutamate, 40 mM KF, 10 mM Tris-HCl, pH 7.2, to 0.98 Osm/kg with sucrose internal solution, and bathed in 480 mM Tris, 10 mM KCl, 10 mM $CaCl_2$, 50 mM $MgCl_2$, pH 7.6, external solution; then both sides of the axon were made hyperosmotic to 1.4 Osm/kg with solutions containing added sucrose. Conductance was measured (*diamonds*). Both solutions were exchanged with those of 3.6 Osm/kg, with added sucrose, and conductance was measured again (*solid circles*). The axon was then perfused with the 1.4 Osm/kg solutions, and conductance again measured (x). Introduced into Eq. 4, the ratio of conductances here in 1.4 and 3.6 osmolar solutions gives an estimate of 1,310 ± 7 Å^3 (N = 50) for the increase in sucrose-inaccessible space upon channel opening. The 3.6 Osm/kg data, rescaled to match the 1.4 Osm/kg data at high voltage, shows no shift in th G-Ψ curve (*open circles*). This data is redrawn with a series resistance correction in Figs. 10 *a* and 11.

With sorbitol as the stressing agent rather than sucrose, conductance again was suppressed (Fig. 5 *a*) and showed no shift in the voltage dependence (Fig. 5 *b*).

Limiting conductance vs. applied stress

The changes in potassium conductance at saturating voltage (the average of measured values at +60, 70, and 80 mV) as a function of osmotic stress are summarized in Table 1 and Fig. 6. Consistent with Eq. 4, the logarithm of the ratio of limiting conductances is roughly linear in differences in applied osmotic stress. These data will be used below to compute the change in the channel's internal aqueous volume.

Channel kinetics

To study the slowing of the potassium channel response in hyperosmotic solutions, we fitted sucrose and sorbitol

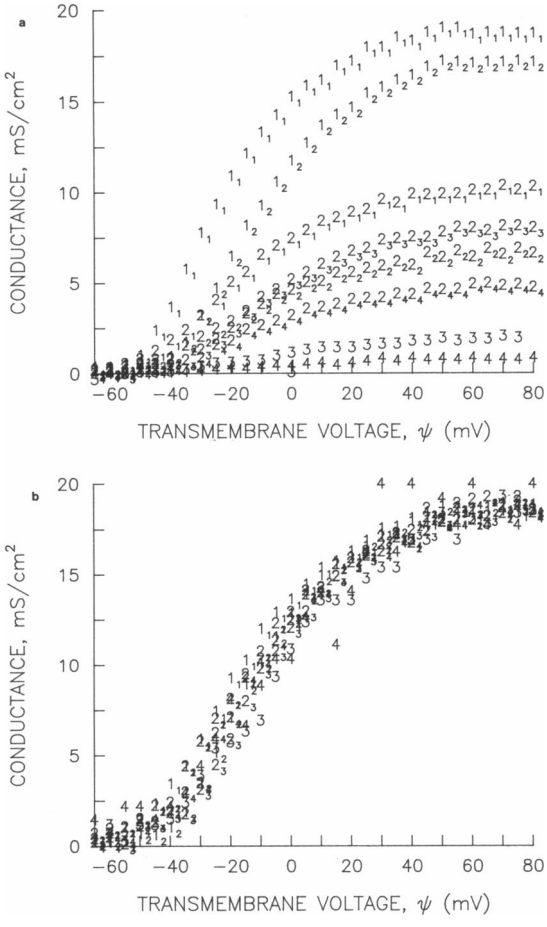

FIGURE 5 A much-abused axon forced to suffer exposure to a series of solutions made hyperosmotic with sorbitol (*a*). The numbers 1, 2, 3, and 4 are molarities of sorbitol in the solutions, with respective osmotic pressures 2.1, 3.1, 6.3, and 11.2 Osm/kg. Subscripts refer to the first, second, third, fourth exposure to a particular solution. The actual sequence of application was: 1-2-3-4-2-1-2-3-2. As one would expect, there is some deterioration of the K conductance, but the rescaled data (*b*) superpose remarkably well. "Instantaneous" conductance and pulse as in Fig. 4.

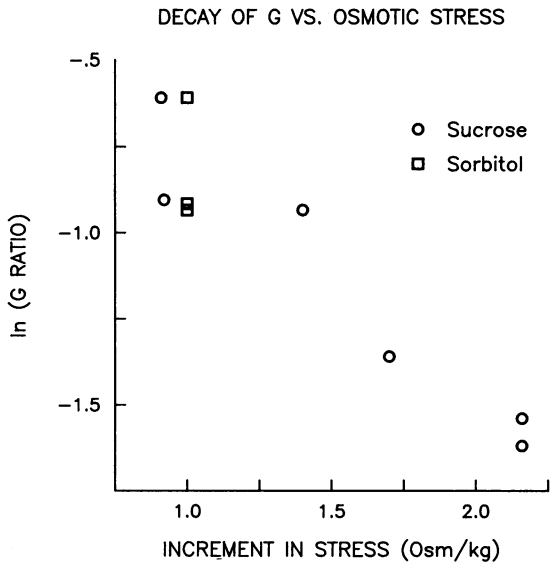

FIGURE 6 Test of the expected linear relation between log *G* ratios and increment in applied osmotic stress. The slope can give an estimate of the volume of water that must leave the bathing solutions in order for the channels to open, Eq. 4. Note agreement between data collected with sucrose and sorbitol hyperosmotic solutions.

data with a single exponential. Hyperosmotic solutions seem to decrease the on rate (increase τ_{on}) much more than they decrease the off rate. This slowing of gating kinetics had been observed before (Shoukimas et al., 1981). Since on and off rates are neccessarily measured at very different voltages, changes in kinetics with osmotic stress cannot be used to measure changes in steady-state conductance. For this reason, we will not consider kinetics in our analysis of the foregoing data.

Selectivity under stress

One characteristic of the squid delayed rectifier is its selectivity among alkali cations (Armstrong, 1975; Yellen, 1987). We examined this selectivity under the action of hyperosmotic solutions to see if there were some osmotic response of the open pore. Perfused, tetrodotoxin-treated axons were kept in an external solution of 200 mM KCl while the internal solution was changed from 200 mM KCl to 200 mM RbCl, then to 200 mM NH_4Cl, and finally back to 200 mM KCl. Within each pair of cations, we perfused solutions with the same ionic activities but various osmotic pressures, then stepped the holding potential from −90 to various test potentials. Electrode junction potentials were measured in a chamber without an axon for most solutions used. They ranged from +11.4 to +12.6 for all solutions tested, and were subtracted from measured potentials to give the net values tabulated below.

Internal solution	Π_{osm}	Reversal potential	*G*
	Osm/kg	*mV*	*mS/cm²*
Rb	0.98	+7	47
	2.2	+8, 8.8	23.4
	3.5	+7	6
	1.52	+9.8	
NH_4	1.56	+50, 54, 55	
	3.5	+55, +55	

No change in selectivities with osmotic stress, measured as biionic potentials, was seen between K, Rb, and NH_4

TABLE 1 Osmotic stress, conductivity, limiting *G*

Agent	Π_{oxm}	γ Int	γ Ext	G	G ratio	γ ratio Int	γ ratio Ext
	osm/kg	*mS/cm*					
Sorbitol	2.1	5.45	13.2	18.75			
	3.1	2.5	8.05	10.2	1.84	2.18	1.64
(Fig. 5)							
	3.1	2.5	8.05	6.9			
	2.1	5.45	13.2	17.2	0.40	0.61	0.46
	2.1	5.45	13.2	17.2			
	3.1	2.5	8.05	8.1	2.12	2.18	1.64
Sucrose	0.99	8.8	28.0	47.0			
	1.9	4.85	15.0	23.4	2.01	1.81	1.86
	1.9	4.85	15.0	23.4			
	3.6	2.05	6.1	6.0	3.90	2.37	2.46
Sucrose	1.44	6.6	20.2	24.8			
	3.6	2.05	6.1	4.9	5.06	3.22	3.31
(Fig. 4)							
	3.6	2.05	6.1	4.9			
	1.44	6.6	20.2	22.8	0.21	0.31	0.30
Sucrose	0.98	8.8	28.0	23.0			
	1.9	4.85	15.0	9.3	2.47	1.81	1.86
(Fig. 3)							
	1.9	4.85	15.0	9.3			
	3.3	2.54	7.67	3.65	2.55	1.91	1.96

Isotonic external control (Fig. 7 *b*)	
Tris	26.0
Sorbitol	10.0
Sucrose	8.1

The measured osmotic stress Π_{osm} for each solution is given in osmoles/kilogram (1 Osm/kg = 22.4 atmospheres, 1 atm = 1.01×10^6 dyne/cm^2 = 1.01×10^5 N/m^2). Solution conductivities γ are given in milliSiemens/centimeter. The G here are the K conductances measured as described in the text. The ratios of G or γ are for successive pairs of internal and external solutions applied to the same axon; G ratios and γ ratios are as plotted in Figs. 6 and 12 except that the inverse ratio was used for downward steps in sorbitol or sucrose concentration.

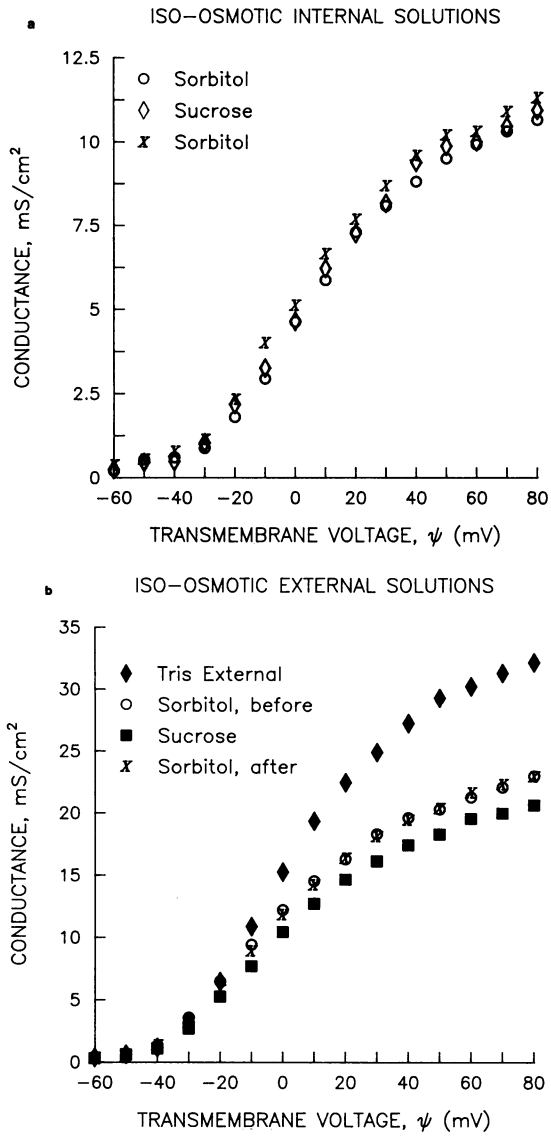

FIGURE 7 Response to isoosmotic solutions (0.98 Osm/kg). (*a*) Internal solutions. (*b*) External solutions. Conductance vs. voltage data in a set of isoosmotic solutions composed of different solutes and of necessarily different conductivities and channel blocking capabilities. Sensitivity to external rather than internal solution suggests to us some impedance on exiting K ions rather than a blocking action by the osmotic agents. Voltage pulse pattern as in Figs. 2 and 5. Internal conductivities are 8.5 mS/cm sorbitol, and 6.7 mS/cm sucrose. External conductivities are 26 mS/cm Tris, 10 mS/cm sorbitol, and 8.1 mS/cm sucrose.

solutions, even at 3.5 Osm/kg, despite the suppression of limiting potassium currents. Selectivities agreed qualitatively with earlier estimates (Bezanilla and Armstrong, 1972; Wagoner and Oxford, 1987).

Isoosmotic stress

To distinguish between the action of osmotic stress and the effects of solution conductivity or solute blockage suppressing G, we compared results from successive solutions of identical (*a*) osmotic stress or (*b*) conductivity.

The data in Fig. 7, *a* and *b* show axonal response to "isoosmotic control" solutions of the same osmotic stress but different internal or external solution conductivity. Any change in G here must be associated with some nonosmotic mechanism. Isoosmotic internal solutions of sorbitol and sucrose, *of different conductivities*, 8.5 and 6.7 mS/cm, respectively, did not affect current when exchanged intraaxonally (Fig. 7 *a*). However, the axonal response to different isoosmotic external solutions did create changes that seem to correlate with bulk solution conductivity, 26, 10, and 8.1 mS/cm for Tris, sorbitol, and sucrose, respectively. In the Discussion, we suggest

that this deviation may be accounted for in terms of a modified series resistance of the Schwann cell layers.

Another set of control solutions had identical conductivities but different osmotic pressures. These did effect a net change in K conductance in quantitative agreement with results using other stressing solutions. Because the axon deteriorated before a return to the original solutions, the data from these controls were not used for volume computation.

Hypoosmotic stress

If channels are always under osmotic stress, then *hypoosmotic* solutions should favor the open state of the channel. According to the data in Fig. 8, by decreasing solution osmoticity to 0.835 Osm/kg, one observes reversibly *increased* K conductance.

DISCUSSION

We will argue that these results suggest at least three qualitative features of squid giant axon potassium channels.

(*a*) The changes in state that occur in response to applied voltage seem to be only weakly connected to the osmotically sensitive act of opening.

(*b*) Upon opening, some 40–50 molecules of water appear to associate with regions of the channel inaccessible to solute.

(*c*) This ion-specific channel is always under functionally significant osmotic stress whose relaxation by hypoosmotic solutions might even increase macroscopic potassium conductance.

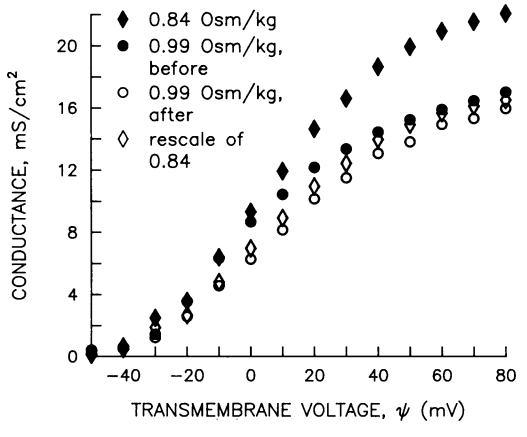

FIGURE 8 Squid axon potassium conductance increases reversibly in hypoosmotic solutions. The observed increase is not in proportion to solution conductivity. Voltage pulse as in Figs. 4 and 5. There is no obvious shift in voltage dependence.

Volume computation

According to Eqs. 3 and 4, the change in the logarithm of the conductance G with change in osmotic stress Π_{osm} is a function of the volume of water Δv entering the channel upon opening. To ensure that we compute this volume under conditions where there is no variation of G with applied voltage, we have examined the action of osmotic stress on limiting conductances at saturating voltage. This information has been summarized in Fig. 6 and Table 1. Each point in Fig. 6, the log of a ratio of limiting conductances for two different osmotic stresses applied to the same axon, gives a volume estimate that can be found from a numerical solution of Eqs. 3 and 4. These Δv values are tabulated in Table 2. Details of the computation are given in the Appendices, where we develop sequential and parallel models for a family of voltage-dependent closed states and an osmotically sensitive opening step. For a parallel model, the volumes are calculated by Eq. 4, and are identical to the sequential model result when $A = 0$ (Table 2).

These computations suggest that there is a water volume Δv of 1,350 ± 200 Å^3 that moves with channel

TABLE 2 Computed volume changes

Agent	Π_{osm}	Π_1/Π_2	G	G_2/G_1	Δv ($A = 0$)	Δv ($A = 5$)
	Osm/kg				*Å³*	
Sorbitol	2.1		18.75			
(Fig. 5)	3.1	0.68	10.2	0.544	1070	1580
	3.1	0.68	6.9	0.401	1580	2000
	2.1		17.2			
	2.1		17.2			
	3.1	0.68	8.1	0.471	1320	1790
Sucrose	0.99		47.0			
	1.9	0.52	23.4	0.5	1320	2307
	1.9		23.4			
	3.6	0.53	6.0	0.256	1400	1822
Sucrose	1.44		24.8			
(Fig. 4)	3.6	0.4	4.9	0.198	1300	1820
	3.6	0.4	4.9	0.215	1240	1760
	1.44		22.8			
Sucrose	0.98		23.0			
(Fig. 3)	1.9	0.52	9.3	0.404	1730	2680
	1.9		9.3			
	3.3	0.57	3.65	0.392	1150	1650
					$\overline{\Delta v}$ = 1350 ± 200	1930 ± 350

Volume changes Δv were found by numerical solution of Eq. 3 in Methods for A values derived from the models described in Appendix 1 and the methods of solution described in Appendix 2. The smaller Δv's ($A = 0$) are a lower limit, the solutions to Eq. 4 in the Methods. These are the results for the parallel model as well. Ratios of Π_{osm} and G are given next to the first or second entry of each pair of solutions depending whether there was a step down or up in applied osmotic stress. The value of thermal energy kT at 10°C is 3.9×10^{-14} ergs. (1 osmol/kg = 22.4 atmospheres = 22.4×10^6 dyn/cm^2). $\overline{\Delta v}$ is given as the mean ± standard deviation.

opening. To derive this volume, we have used the fact that the rescaled hyperosmotic stress data, Figs. 3–5, show an uncoupling of voltage dependence from osmotic stress (the case $A = 0$, Appendix 1). To allow for some coupling by a sequential model would lead to *higher* estimates of channel opening volume, by as much as 45% but most likely by no more than 25–35% ($A = 2$, Appendix 2), and smaller open channel probabilities. The Δv's given in Table 2 then represent a lower limit. (The volumes given in parentheses are expected maximum values when one assumes noticeable $\Psi - \Pi$ coupling, the case for $A = 5$ as described in Appendix 2.) Experiments where sucrose replaced electrolyte while maintaining osmotic activity showed a large shift in voltage dependence (Baker et al., 1964; Moore et al., 1964). The present measurements were done under conditions of strictly maintained ionic strength.

The similarity of the rescaled hyperosmotic stress data (Figs. 3–5) suggests that osmotic stress acts uniformly at all applied voltages and that there was no need to use only limiting conductances at high voltage. G ratios at all voltages have been used to estimate internal volume changes. In 202 volume determinations from five axons, for $A = 0$, giving a lower bound in $\Pi_{osm}\Delta v$, we estimate $\Delta v = 1{,}378 \pm 256$ Å^3.

Most of the variation came from differences between axons. Within the data set from one axon, for example, the variation was <1% (see Fig. 4). This tightness of estimates shows in another way the lack of any shift in voltage dependence.

Blockage vs. conductivity vs. stress

Might the observed decrease in potassium conductance, interpreted by us as a volume change of the sucrose- or sorbitol-inaccessible space, indicate instead blockage of channels by the presumed osmotic agent (or a contaminant thereof)? Alternately, could it be a sign of lowered channel conductance due to decreased ionic mobility in hyperosmotic solutions? The effect of osmotic stress, on the other hand, would be to alter the ratio of open/closed times without changing single channel conductance.

Ideally, one would test the effect of osmotic stress with single-channel measurements similar to those on VDAC in bilayers (Zimmerberg and Parsegian, 1986). Unfortunately, it is not yet feasible to access both sides of an osmotically stressed squid axon while recording single channels. Because we are forced to observe many K channels simultaneously, most of the following discussion deals with questions of interpreting macroscopic data in terms of a microscopic mechanism.

Blocking

It is clearly difficult to rule out a phenomenon as vague as "blocking." For present purposes we define blocking as inhibition of current flow through an open channel. It is difficult to distinguish such blockage from fast flickering of an open channel to a closed state driven by osmotic stress.

To the extent that blockage implies some interaction of specific agents, sucrose or sorbitol in the present instance, with the ionic path, the identical behavior of solutions made from different species (Fig. 7 *a*) argues against sucrose/channel or sorbitol/channel interaction as a source of interference in the outward movement of potassium. (The fact that sucrose and sorbitol are only dimer and monomer of hexose weakens the idea that they are really distinct species, especially if molecules are blocking by inserting their ends; but in isoosmolar solutions the concentrations of sucrose and sorbitol, and thus of their "ends," are quite different.)

Even single-channel measurements will not allow one to rule out the occurrence of "tonic" block due to the interaction of osmotic species both to open and to closed states. Very rapid flickering induced by either osmotic stress or rapid association/dissociation would appear as a decrease in single-channel conductance rather than a change in open/closed ratio.

Solution conductivity

We examined the effects of isoosmotic solutions, media that should exert the same osmotic stress but have different solution conductivities.

Internal conductivity

There was no observed sensitivity to internal solution conductivity (Fig. 7 *a*). The lack of variation of potassium conductance with internal solution conductivity is consistent with K saturation (Wagoner and Oxford, 1987) of the channels; it suggests that ionic diffusion in putative internal vestibules to the K channel is not rate limiting. (A small correction of G for potassium concentration using the data of Armstrong [Begenisich and Lynch, 1974] made negligible difference in estimated volumes.)

External conductivity

There does seem to be an effect of external solution conductivity on the observed G. This is especially clear for the case of an external solution where sorbitol or sucrose is replaced by Tris and chloride ions. One way to rationalize this sensitivity to external, but not internal, solution conductivity is to consider explicitly the series resistance of the Schwann cell layer through which the exiting K

ions must flow (Taylor et al., 1980). We assume that the resistance of this space is inversely proportional to solution conductivity. Any series resistance acts to divide the applied voltage Ψ. This consideration causes one to recognize a shift in the current-voltage curve and consequently in the derived G-voltage curves. By recasting the data of Fig. 8 *b* in this way, we find it possible to reconcile the differences in G vs. voltage (Fig. 9), as long as we postulate a Schwann cell layer resistance of 8 ohm cm^2 for axons in isoosmotic Tris solutions. This value is large compared to the 4–5 ohm cm^2 usually expected (Hodgkin et al., 1952*c*).

However, even at this high initial series resistance, one cannot create a similar overlap of the hyperosmotic data. The effects of the same kind of series resistance transformation on the data of Figs. 4 and 5 are shown, respectively, in Fig. 10. Fig. 11 shows the corrected and original data of Fig. 4 together. Paradoxically, the application of the series resistance correction, to diminish the presumed role of osmotic stress, in fact leads to even greater apparent shifts in conductance with hyperosmotic solutions to correspondingly greater estimates of the internal aqueous volume change.

In addition, one does not see in Figs. 10 and 11 the shifts to the right in voltage dependence expected from a significant external series resistance. It is unlikely that osmotic effects have compensated for such a conductivity shift. Osmotic forces, sucking the channel shut, would if anything cause a further shift to the right. Instead, no shift was seen either here or in the uncorrected data (Figs. 2, 4, 5). It is possible that external conductivity acts to limit ion exit from the channel in a region spatially removed from the voltage sensor, lowering single-channel conductance by a local series resistance without shifting the voltage dependence. Again, the correction based on this mechanism leads to greater changes in conductance with osmotic stress, and an average volume estimate increased by 8%.

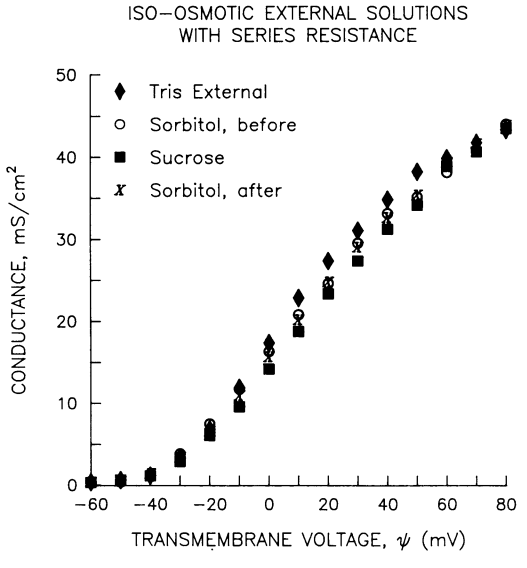

FIGURE 9 Interpretation of the isoosmotic external solution data of Fig. 7 *b* in terms of the effect on the series resistance R_s of the Schwann cell layer. Estimates here used a value of R_s = 8 ohm-cm^2 for axons in the reference Tris external solution (conductivity γ = 26 mS/cm) and made the assumption that R_s is inversely proportional to bulk external solution conductivity (given in Table 1).

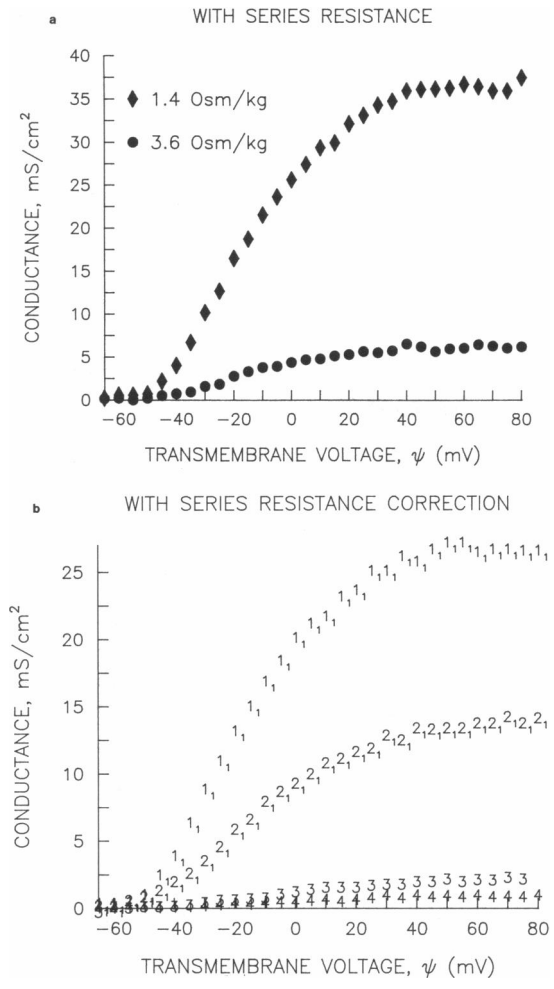

FIGURE 10 Failure of a series resistance model to explain the suppression of G vs. voltage under hyperosmotic stress: (*a* and *b*) data of Figs. 4 and 5 respectively. Estimates here used a value of R_s = 8 ohm cm^2 for axons in the reference isoosmotic Tris external solution (conductivity γ = 26 mS/cm) and made the assumption that R_s is inversely proportional to bulk hyperosmotic external solution conductivity (given in Table 1). The transformation that caused overlap of isoosmotic solution data (Figs. 7 and 9) does not create similar overlap for the hyperosmotic solution data.

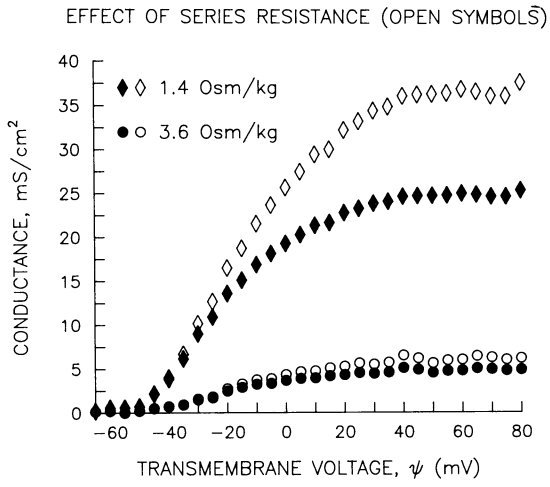

FIGURE 11 Comparison of the data on sucrose-stressed axons with and without transformation for series resistance. Solid symbols are for G plotted as in Fig. 4; open symbols are transformed as in Fig. 10 *a*. The R_s calculated from a Tris R_s of 8 ohm-cm^2 is 10.3 ohm-cm^2 for 1.4 Osm/kg and 34 ohm-cm^2 for 3.6 Osm/kg. The effect of transformation is to increase the ratio of limiting conductances by ~50%. This would lead to ~40% higher estimates of internal aqueous volume change.

Correlation of G and external solution conductivity

In Fig. 12 we have plotted the ratio of limiting G vs. ratios of external solution conductivities to see if there is some empirical correlation. Indeed, the data from the hyperosmotic preparations do show a proportionality, but the slope is not equal to unity. We suspect that this correlation indicates a real (negative) correlation between solution conductivity and solution osmotic pressure, both of which depend on sorbitol or sucrose concentration. Besides, there is a completely different relation between G and the conductivity of isoosmotic external solutions. We therefore feel justified at this stage interpreting changes of macroscopic G induced by sucrose and sorbitol in terms of osmotic stress.

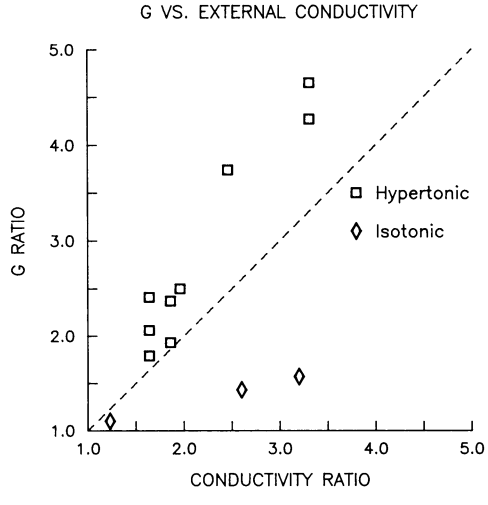

FIGURE 12 Ratio of K conductance vs. ratio of external solution conductivities. Correlation of hyperosmotic solution data probably reflects dependence of both conductivity and G on sucrose or sorbitol concentration rather than the direct relation that would follow the slope of the dashed line. The correlation with isoosmotic solution data bears no resemblance either to the hyperosmotic case or to the ideal dashed line.

Volume changes during channel opening

The estimated volume change is large, comparable to those of total channel water volume. If we take a cross-sectional area of 3 × 3 Å^2 from cation sieving (Bezanilla and Armstrong, 1972), and a length of 100 Å to take into account membrane thickness and some extension from the host membrane, we estimate a total volume of only 900 Å^3. (Of course, the 3 × 3 filter need be only a short part of the total channel path.) A cylindrical channel of wider (8 Å diameter) opening such as would be blocked by TEA (Armstrong, 1975), even over a length of 30 Å, would have a volume similar to what we measure (1,365 Å^3). The mechanism of closing such a channel might be more like a squeeze, or the macromolecular rotation suggested for gap junctions (Unwin and Ennis, 1984) rather than a gate or flap.

For VDAC too, the conformational changes in the protein assocated with gating led to a significant movement of water relative to the size of the channel (Zimmerberg and Parsegian, 1986). There, a change in diameter from 40 down to 20 Å could explain the volume change. (Because VDAC has a large "closed" conductance, there is still a lot of room for water in the channel.)

We repeat here the obvious point that the sucrose- or sorbitol-inaccesible space need not be identical with the volume through which the ions actually pass. In a structure as elaborate as a squid axon, there are many regions that can respond to osmotic stress. It is quite possible that channel vestibules contain space that is accessible to sucrose or sorbitol in the open state and inaccessible in the closed state. Our measured Δv is a net volume change. (This kind of caveat applies equally to measures of the "gating charge" Q that moves in response to an externally applied voltage. Both Q and Δv are operationally defined quantities reflecting artificially induced changes in the condition of the channel.) Moreover, it is possible that osmotic stress shifts steady-state potassium inactivation. However, the calculated volume change was the same when axons were subjected to a subtracting holding potential of −130 mV instead of −100 mV, the usual subtracting holding pulse (1,470 ± 340 Å^3, n = 16). Generally, in the squid axon, there is always the possibil-

ity of states or factors which we presently do not even imagine which are responsible for the effect of hyperosmotic solutions.

Channel opening and hydration

Unlike VDAC, the closed K channel has no measurable conductance. The complete or near-complete dehydration of at least some part of the channel suggests that surface hydration forces such as have been seen to dominate the close approach of membranes or macromolecules (Rau et al., 1984; Gruner et al., 1986; Parsegian, 1982; Parsegian et al., 1986; Rand, 1981) might be a significant, even dominant, force in channel closure. One may imagine an internal channel surface experiencing both repulsive and attractive hydration forces that govern the transition between open and closed conformations. The effect of applied voltage, then, might be to disturb this competition of attractive and repulsive forces by moving polar groups, dipoles or charges.

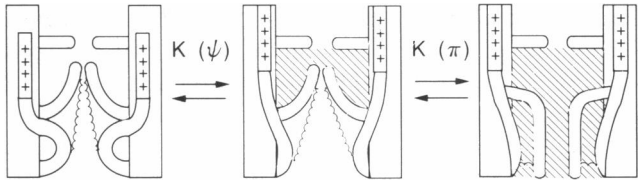

FIGURE 13 A spring-loaded channel. One might consider a spring between a voltage-dependent "gate" and an osmotically-sensitive channel. The channel "gates" are sensitive to voltage but the actual opening is osmotically sensitive. The ~20 kT or ~12 kcal/mol energy of gating is very large compared to the osmotic work ~kT or ~0.6 kcal/mol. Open gates allow the osmotically-dependent opening step. The cross-hatched region is the solute-inaccessible space. We imply in this drawing that the solute-inaccessible volume of a vestibule changes during opening, but this is only one possibility. The model is meant to satisfy the observation that osmotic factors do not appear to affect the voltage dependence of gating, but gate opening in itself is not enough to allow K to flow. This drawing corresponds to a sequential model. For a parallel model, the two sets of flaps would be physically separated and fluctuate independently. (Cartoon after a model by Bob Guy.)

Models

For concreteness, we have considered the absence of shift in voltage dependence of osmotically stressed channels (Figs. 2, 4, 5) in the light of both CC_nO and parallel models. These are the simplest schemes that seem to describe the steady-state channel behavior. Lack of shift of voltage dependence require sequential models to have a number of closed states so that the necessary redistribution of closed states be lost in the noise of the measurement (Appendices). The "gating" process involves a redistribution of closed states under the action of applied voltage, effecting the displacement of an apparent "gating" charge Q. The measured work of moving such charge over a range of applied voltage amounts to some 20 kT (White and Bezanilla, 1985) and is far greater than the ~kT energy that is available from the osmotic work of moving ~1,350 cubic Å^3 of water under an osmotic driving force of 0.98 Osm/kg or 22 atmospheres. There can be only a weak coupling between the structural changes associated with channel opening and those processes responsive to voltage. The differential action of hydrostatic pressure on Na channel gating vs. opening (Conti et al., 1982) and a similar distinction seen in heavy water replacement experiments (Schauf et al., 1982) both suggest that gating charge displacement and physical opening of the ionic path are two distinct events.

Imagine (Fig. 13) that the voltage-driven parts of the channel protein are connected by a relatively weak spring to the part that actually opens to form an aqueous path. The step of opening is helped by tension developed in the spring, but it is inhibited by the work of drawing water into the actual channel. This reluctance to open, even after movement of gating charges, is consistent with single channel recordings (Conti and Neher, 1980; Llano et al., 1988) where, despite the application of voltage that corresponds to maximum average ion flux, the channel is *not* open all the time but continues to flicker. However, the lack of effect of osmotic stress on selectivity (see Results) suggests that the open channel, or at least any "selectivity filter", is not itself susceptible to osmotic stress.

Note that voltage-independence of the final step in opening a channel is consistent with activation continuing to speed up beyond the voltage where conductance reaches its limiting value if the rate-limiting reaction is voltage-dependent and the opening step rapid.

One could even imagine two independent events, one the movement of a lid or cap or gate connected with the movement of gating charge, and another that involves closing of the channel by stress working against some spring whose tension is independent of the position of the charged gates (Ofer Eidelman, personal communication). This is developed in Appendix 1 as a parallel model.

It is of course possible as an alternative hypothesis that the open channel itself responds to osmotic stress by decreasing in volume and that the decrease in macroscopic G corresponds to a decrease in single-channel conductance. Again, there will be a solute-inaccessible volume lost under stress. To estimate this volume would require some assumption not only about the osmotic stress but also about the relation between net channel conductance and channel volume. Given the limited information available, we expect that single channel deformation is unlikely. First, results on the insensitivity of channel selectivity with applied stress suggest that there is little

deformation under stress, at least of the "filter" region. Second, as pointed out in the Introduction, even channels working in "normal" isoosmotic solutions are under a stress (~1 Osm/kg) of excluded species. If the osmotic opening energies are $\sim kT$ as is suggested by the response to 2–4 Osm/kg solutions, then open-state single-channel conductances should vary rather than exhibit a fixed value. However, this is not the case (Llano et al., 1988). Rather, they would have been seen to vary, because it would take only $\sim kT$ of energy to perturb them. We expect, therefore, that the open-state channel structure is reasonably stable against the level of osmotic stress we have applied in this study.

One should recognize that what is seen as single-channel conductance can be an average over very rapidly "flickering" transitions between short-lived open and closed states, although there is no evidence at the present for such fast flickering for the potassium channel of the squid axon. The instrument-averaged apparent single-channel conductance will be less than the maximal conductance. Osmotic stress, increasing the probability of a closed-flickering configuration, would then create the appearance of lower single channel conductance.

Recognition of the action of osmotic stress automatically suggests why it is possible to increase specific K conductance by the relaxation of stress (Fig. 8), although these data are also consistent with tonic block from isoosmotic solutions. These data underscore the likelihood that selective channels are always under some kind of osmotic stress due to exclusion of solutes. We suggest that this stress of exclusion can be an important feature of controlled ionic conductance, a sensitivity to solute environment that provides greater flexibility in channel response than has been suspected hitherto.

APPENDIX 1: MODELS OF CHANNEL OPENING

We consider the possibility of the channel protein occupying one of several states $\{i\}$ whose energies $\{\mu_i\}$ are a function of applied voltage Ψ and osmotic stress Π_{osm}. The probability p_i of being in a particular state is proportional to $\exp(-\mu_i/kT)$.

To put the μ_i in a form appropriate for variation in applied Ψ and Π_{osm}, we write

$$\mu_i = \mu_i^0 + \Psi Q_i + \Pi_{osm} v_i.$$

Here, v_i is a volume of water associated with the channel i and inaccessible to osmotically active species outside. Q_i is that charge configuration that interacts with the applied voltage. ($\bar{Q} = \Sigma Q_i$ is the "gating charge".)

Direct-coupling model

For the simple Closed ↔ Open kinetics of VDAC,

$$\mu_{open} = \mu_{open}^0 + \Psi Q_{open} + \Pi_{osm} v_{open}$$

and

$$\mu_{closed} = \mu_{closed}^0 + \Psi Q_{closed} + \Pi_{osm} v_{closed}.$$

Then the ratio

$$(open)/(closed) = (O/C) = \exp[-(\mu_O - \mu_C)/kT]$$

can be written

$$(O/C) = \exp\{[-(\mu_o^0 - \mu_c^0) - \Psi(Q_o - Q_c) - \Pi_{osm}(v_o - v_c)]/kT\}.$$

This can be put in a more familiar form by writing the difference in charges $Q_o \times Q_c = nq$, the difference $\mu_o^0 - \mu_c^0 = -nq\Psi_0$ and $v_o - v_c = \Delta v$. Then

$$(O/C) = \exp\{[-nq(\Psi - \Psi_0)/kT - \Pi_{osm} \cdot \Delta v]/kT\}.$$

It is worthwhile to recognize explicitly that the quantity $\mu_o^0 - \mu_c^0 = -(nq\Psi_0)$ is the work required to go from the closed to the open state in the absence of applied voltage Ψ. Because, for VDAC, this work strongly favors the open state, only when we apply sufficient voltage Ψ to change the work of opening do we see what $nq\Psi_0$ actually is.

In the case of VDAC, the transition step is a function simultaneously of both Π_{osm} and Ψ. Applied osmotic stress has the effect of shifting the current-voltage curve.

Multiple state models

Sequential model

In the case of the K channel studied in this paper, there is most likely a family of closed states sensitive to Ψ but not Π_{osm} and an osmotically sensitive transition to one or more open states.

$$C_0 \underset{K_1(\Psi)}{\leftrightarrow} C_1 \underset{K_2(\Psi)}{\leftrightarrow} \cdots \underset{K_{n-1}(\Psi)}{\leftrightarrow} C_{n-1} \underset{K_n(\Psi)}{\leftrightarrow} C_n \underset{K_\pi(\Pi_{osm})}{\leftrightarrow} O.$$

If the final transition $C_n \leftrightarrow O$ has little associated gating charge movement, then we can think of the channel as having a lumped closed state C_0 within which occurs its gating with voltage.

$$C_0 \underset{K_\psi(\Psi)}{\leftrightarrow} C_n \underset{K_\pi(\Pi_{osm})}{\leftrightarrow} O.$$

In this scheme

$$K_\psi = (C_n)/(C_0) \text{ or } (C_0) = (C_n)/K_\psi$$

and

$$K_\pi = (O)/(C_n) \text{ or } (O) = K_\pi(C_n).$$

Because for the squid axon one measures a macroscopic conductance, and one assumes that the closed channels are really closed, the observed conductance is proportional to the number of open channels, and the fractional conductance is proportional to the fraction of channels that are open. This fraction can now be written

$$\frac{(O)}{(C_0) + (C_n) + (O)} = \frac{K_\pi(C_n)}{[(C_n)/K_\psi] + (C_n) + K_\pi(C_n)} = \frac{K_\pi}{(1/K_\psi) + 1 + K_\pi}.$$

The ratio $(C_n)/(C_0) = K_\Psi$ is related to an electrical work of shifting charge nq as

$$K_\psi = \exp[nq(\Psi - \Psi_0)/kT].$$

Here the quantity $nq\Psi_0$ denotes the electrical work needed at zero applied voltage to go from a state C_0 corresponding to no shift in gating charges to the state C_n, where all charges have been fully displaced. (In this sense, it is analogous to the Ψ_0 used above for the difference in μ^0 work for the electrical work).

The need for an additional $C_n \leftrightarrow O$ opening step adds to the actual work of opening and creates a difference between Ψ_0 and that apparent Ψ_0^{app} where macroscopic conductance has reached half its maximal value (see for example Fig. 4 in White and Bezanilla [1985]). We may think of a quantity $nq\,\Psi_0^{app}$ as an actual work of opening $-kT \ln K_\pi$. In the presence of an osmotic work $\Pi_{osm} \cdot \Delta v = W_\pi$, we can then write the equilibrium constant K_π for the channel-opening step

$$K_\pi = A \exp(-\Pi_{osm} \cdot \Delta v/kT) = A \exp(-W_\pi/kT),$$

where $-kT \ln A$ is the nonosmotic work involved in the opening step.

The fraction of open states can now be written in the form

$$\frac{K_\pi}{(1 + K_\pi) + (1/K_\psi)} = \frac{K_\pi/(1 + K_\pi)}{1 + \{1/[K_\pi(1 + K_\pi)]\}}.$$

K_ψ, the equilibrium constant between closed states C_n and C_0, becomes an apparent quantity,

$$K_\psi^{app} = K_\psi(1 + K_\psi).$$

This apparent K_ψ^{app} will show a Ψ_0^{app} different from the Ψ_0 of the gating step alone. In analogy to the relation between Ψ_0 and K_ψ, we write

$$nq(\Psi - \Psi_0^{app}) = kT \ln K_\psi^{app} = kT \ln K_\psi + kT \ln(1 + K_\pi) = nq(\Psi - \Psi_0) + kT \ln[1 + A \exp(-W_\pi/kT)],$$

or

$$\Psi_0^{app} = \Psi_0 - (kT/nq) \ln[1 + A \exp(-W_\pi/kT)].$$

In 0.98 Osm/kg solution (osmotic stress 22.4×10^6 dynes/cm^2) and anticipating a change in channel volume of 1,500 Å^3, $W_\pi \cong kT$ (3.9×10^{-14} ergs). Using the fact that kT/q is ~25 mV, and the literature estimate of $n = 4$ gating charges (Hodgkin and Huxley, 1952*d*, White and Bezanilla, 1985), one may expect Ψ_0^{app} to differ from Ψ_0 by

$$(kT/nq) \ln[1 + A \exp(-W_\pi/kT)] \simeq 6.5 \ln[1 + (A/e)].$$

However, this last statement assumes that the number of responding gating charges at Ψ_0 is close to that at the empirical Ψ_0^{app}. In fact, it has been shown by White and Bezanilla (1985) that most gating charges have been shifted at voltages which give half-maximal conductance. It may be more accurate to introduce $n = 1$ or 2 into this last equation (which would necessitate the introduction of more than two closed states in a sequential model.)

The noise in the rescaled data of Figs. 3–5 allow one to imagine a voltage shift of 5 mV at the most so that $\ln(1 + A/e) \leq 1$ or $A \leq e^2 - e < 5$. To be cautious in interpretation, we have used a range of $A = 0$ to 5 for our volume estimates, to be consistent with no significant voltage shift in our data. (Literally, a value of $A = 0$ means that a channel will never open!) A small value for A is suggested by the (limited) information available on single channel observations (Conti and Neher, 1980; Llano et al., 1988); this point is developed further in Appendix 2.

One may imagine the existence of a weak spring between a massively powerful gating mechanism and the channel itself. An "open" position (state C_n) of the first only tugs at the channel which still requires an additional, osmotically sensitive, energy E_0 to open. A "closed" position (C_0) of the gating mechanism prohibits channel opening altogether. But the energy required to move the gating mechanism is always much larger than that exerted through the spring, so the response to voltage is virtually independent of the spring tension. The voltage dependence of channel opening is virtually the same whether or not the channel is osmotically stressed. This insensitivity is apparent in all our measurements.

Parallel model

Because the known gating energies and open channel conductances described above constrain the open probability for a single channel to be rather small, it is useful to consider an alternative model, in which no sequential coupling is postulated between the voltage-sensitive conformational changes and the osmotically-sensitive conformational changes. Rather, two sets of equilibria coexist in

parallel:

$$G_C \underset{K_\psi(\Psi)}{\longleftrightarrow} G_O$$

$$\Pi_C \underset{K_\pi(\Pi_{osm})}{\longleftrightarrow} \Pi_O.$$

Both the fully displaced, gating charge–driven conformational change, from G_C to G_O, *and* the osmotically-sensitive transition from Π_C to Π_O are needed for ion flux, through two gates in series. Only $G_O\Pi_O$ conducts. In this scheme, the probability of opening is the product of two independent probabilities, that of populating G_O and that of the osmotically-sensitive transition.

APPENDIX 2: METHOD FOR COMPUTING VOLUME CHANGE Δv

Sequential model

We begin with Eq. 3 of Methods for the ratio of conductance,

$$r = G_2/G_1, \tag{A2.1}$$

measured in solutions of different osmotic pressures Π_2 and Π_1. By defining

$$y_1 = \exp(-\Pi_1 \cdot \Delta v/kT),$$

and

$$y_2 = \exp(-\Pi_2 \cdot \Delta v/kT) = y,$$

Eq. 3 becomes

$$r = \frac{y_2}{y_1}\frac{1 + A\,y_1}{1 + A\,y_2}. \tag{A2.3}$$

For a ratio of pressures

$$p = \Pi_1/\Pi_2, \tag{A2.4}$$

$$\begin{aligned} y_1 &= \exp(-\Pi_1 \cdot \Delta v/kT) \\ &= \exp(-p\Pi_2 \cdot \Delta v/kT) \\ &= y_2^p. \end{aligned} \tag{A2.5}$$

We rewrite Eq. A2.1 as

$$r = \frac{y}{y^p}\frac{1 + Ay^p}{1 + Ay} \tag{A2.6}$$

or

$$A(r - 1)\,y^p + ry^{p-1} - 1 = 0. \tag{A2.7}$$

We solve Eq. A2.7 numerically for y using measured conductance ratios r and osmotic stress ratios p for assigned values of A, the osmotically insensitive part of the opening step (cf. Eq. 1 in Methods).

According to the last equation of Appendix 1, any shift in apparent Ψ_0 of channel opening is a function of A,

$$(kT/nq)\ln[1 + A\exp(-E_0/kT)] \cong (25/n)\ln(1 + A/e). \tag{A2.8}$$

The rescaled data of Figs. 3–5 suggest that this shift is ≤5 mV so that $\ln(1 + A/e) \le 5/6.5$, $A \le 5$ for $n = 4$ or $\ln(1 + A/e) \le 5/25$, $A \le 0.5$ for $n = 1$. This last value would suggest that single channels open only 20% of the time for $W_\pi \approx kT$.

Complete superposition of the rescaled data corresponds to $A = 0$ in which case Equation (A2.6) reduces to

$$r = y^{1-p}. \tag{A2.9}$$

Taking the logarithm of both sides one has

$$\ln r = \ln(G_2/G_2) = -\frac{\Pi_1 - \Pi_2}{kT} \cdot \Delta v, \tag{A2.10}$$

which is the same as Eq. (4) in Methods. The volume changes computed by this equation are minimum values compared to those for very small A. It is these values that are listed in Table 2.

For $A = 5$, an upper limit judging from the rescaled G vs. voltage, the estimated volumes of opening are some 40% larger than the minimal value. These inflated values are given in parentheses in Table 2.

The mean value $\overline{\Delta v} = 1{,}350$ Å^3 suggests that even in normal 0.98 Osm/kg solutions there will be an osmotic work $\Pi \cdot \Delta v \cong 3/4\ kT$. From the flickering of single channels at full depolarization in normal solutions one knows that

$$(O)/(C_n) = A\exp(-\Pi \cdot \Delta v/kT) \cong 1 \text{ or } A \cong 2.$$

If we iterate with this value of A, we now compute a volume some 25% higher that the minimal value, i.e., obtain a $\Delta v = 1700$ Å^3 where $\Pi \cdot \Delta v/kT \cong 0.93$ or $A \cong 2.5$. The single channel data, rough as they are, suggest that A lies between 2 and 3. The Δv estimated with these values of A are ~ 25–35% greater than those for $A = 0$ and lie midway between the limits given in Table 2.

Parallel model

Alternatively, we can use Eq. 4 to calculate Δv. In the limit of maximal gating charge movement, all voltage-dependent equilibria in Scheme A1 lie far to the right, and all channels exist as closed ($G_O\Pi_C$) and open ($G_O\Pi_O$).

The remaining equilibrium,

$$G_O\Pi_C \underset{K(\Pi_{osm})}{\longleftrightarrow} G_O\Pi_O,$$

yields the two-state result, and $K = G_O\Pi_O/G_O\Pi_O = A \exp(\Pi_{osm} \cdot \Delta v/kT)$, $r = y_2/y_1$, and

$$\ln r = \ln(G_2/G_1) = -\frac{\Pi_1 - \Pi_2}{kT} \cdot \Delta v.$$

This is the same as Eqs. 4 and A2.10, and the case where $A = 0$, except there is no constraint on single-channel open probability, reported to range from 30 to 90% (Llano et al., 1988).

We thank Olaf Anderson, Ted Begenisich, Franco Conti, Gerry Ehrenstein, Alan Finkelstein, Robert French, Bob Guy, Ramon Latorre, John Moore, and Fred Sachs for useful discussions. We particularly acknowledge the suggestion by Ofer Eidelman that these data can be described in terms of spatially distinct osmotic and electrical gates.

Support was provided by National Institutes of Health grant GM30376 to F. Bezanilla.

Received for publication 11 July 1989 and in final form 27 November 1989.

REFERENCES

Armstrong, C. M. 1975. Ionic pores, gates, and gating currents. *Q. Rev. Biophys.* 7:179–210.

Baker, P. F., A. L. Hodgkin, and T. I. Shaw. 1962. Replacement of the axoplasm of giant nerve fibres with artificial solutions. *J. Physiol. (Lond.).* 164:330–337.

Baker, P. F., A. L.Hodgkin, and M. Meves. 1964. The effect of diluting the internal solution on the electrical properties of a perfused giant axon. *J. Physiol.* 170:541–560.

Begenisich, T., and C. Lynch. 1974. Effects of internal divalent cations on voltage-clamped squid axons. *J. Gen. Physiol.* 63:675–689.

Bezanilla, F., and C. M. Armstrong. 1972. Negative conductance caused by entry of sodium and cesium ions into potassium channels of squid axons. *J. Gen. Physiol.* 60:588–608.

Bezanilla, F., and C. M. Armstrong. 1977. Inactivation of the sodium channel. I. Sodium current experiments. *J. Gen. Physiol.* 70:549–566.

Bezanilla, F., R. E. Taylor, and J. M. Fernandez. 1982. Distribution and kinetics of membrane dielectric polarization. I. Long-term inactivation of gating currents. *J. Gen. Physiol.* 79:21–40.

Cole, K. S., and J. H. Moore. 1961. Dynamic ion current in the squid giant axon: dynamic characteristic. *Biophys. J.* 1:161–202.

Conti, F., and E. Neher. 1980. Single channel recordings of K^+ currents in squid axons. *Nature (Lond.).* 285:140–143.

Conti, F., R. Fioravanti, J. R. Segal, and W. Stuhmer. 1982. Pressure dependence of the potassium currents of the squid giant axon. *J. Membr. Biol.* 69:35–40.

Ehrenstein, G., and D. L. Gilbert. 1966. Slow change of potassium permeability in squid giant axon. *Biophys. J.* 6:553–566.

Frankenhaeuser, B., and A. L. Hodgkin. 1956. The after-effects of impulses in the giant nerve fibers of *Loligo*. *J. Physiol. (Lond.).* 131:341–376.

Gilly, W. F., and C. M. Armstrong. 1982. Divalent cations and the activation kinetics of potassium channels in squid giant axons. *J. Gen. Physiol* 79:965–996.

Gruner, S. M., V. A. Parsegian, and R. P. Rand. 1986. Directly measured deformation energy of phospholipid HII hexagonal phases. *Faraday Discuss. Chem. Soc.* 81:29–37.

Hodgkin, A. L., and A. F. Huxley. 1952a. The components of membrane conductance in the giant axon of *Loligo*. *J. Physiol. (Lond.).* 116:473–496.

Hodgkin, A. L., and A. F. Huxley. 1952b. A quantitative description of membrane current and its application to conduction and excitation in nerve. *J. Physiol. (Lond.).* 117:500–544.

Hodgkin, A. L., A. F. Huxley, and B. Katz. 1952c. Measurement of current-voltage relations in the membrane of the giant axon of *Loligo*. *J. Physiol. (Lond.).* 116:424–448.

Hodgkin, A. L., and F. Huxley. 1952*d*. Currents carried by sodium and potassium ions through the membrane of the giant axon of *Loligo*. *J. Physiol. (Lond.).* 116:449–472.

Llano, I., C. K. Webb, and F. Bezanilla. 1988. Potassium conductance of squid giant axon: single channel studies. *J. Gen. Physiol.* 92:179–196.

Moore, J.W ., T. Narahashi, and W. Ulbricht. 1964. Sodium conductance shift in an axon internally perfused with a sucrose and low potassium solution. *J. Physiol. (Lond.).* 172:163–173.

Parsegian, V. A. 1982. Physical forces due to the state of water bounding biological materials: some lessons for the design of colloidal systems. *Adv. Colloidal Interfacial Sci.* 16:49–56.

Parsegian, V. A. 1983. Dimensions of the "intermediate" phase of dipalmitoylphosphatidylcholine. *Biophys. J.* 44:413–415.

Parsegian, V. A., R. P. Rand, and D. C. Rau. 1986. Osmotic stress for the direct measurement of intermolecular forces. *Methods Enzymol.* 127:400–416.

Rand, R. P. 1981. Interacting phospholipid bilayers: measured forces and induced structural changes. *Ann. Rev. Biophys. Bioeng.* 10:277–314.

Rau, D. C., B. Lee, and V. A. Parsegian. 1984. Measurement of the repulsive force between polyelectrolyte molecules in ionic solution: hydration forces between parallel DNA double helices. *Proc. Natl. Acad. Sci. USA.* 81:2621–2625.

Schauf, C. L., and J. O. Bullock. 1982. Solvent substitution as a probe of channel gating in *Myxicola*. Effects of D_2O on kinetic properties of drugs that occlude channels. *Biophys. J.* 37:441–452.

Shoukimas, J. J., R. J. French, P. Belamarich, M. S. Brodwick, and D. C. Eaton. 1981. Changes in microviscosity affect squid axon channel gating. *Biophys. J.* 33:282a. (Abstr.)

Stimers, J. R., F. Bezanilla, and R. E. Taylor. 1987. Sodium channel gating currents. Origin of the rising phase. *J. Gen. Physiol.* 89:521–540.

Taylor, R. E., F. Bezanilla, and E. Rojas. 1980. Diffusion models for the squid axon Schwann cell layer. *Biophys. J.* 29:95–117.

Unwin, P. N., and P. D. Ennis. 1984. Two configurations of a channel-forming membrane protein. *Nature (Lond.).* 307:609–613.

Wagoner, P. K., and G. S. Oxford. 1987. Cation permeation through the voltage-dependent potassium channel in the squid axon. Characteristics and mechanisms. *J. Gen. Physiol.* 90:261–290.

White, M. M., and F. Bezanilla. 1985. Activation of squid axon K^+

channels. Ionic and gating current studies. *J. Gen. Physiol.* 85:539–554.

Yellen, G. 1987. Permeation in potassium channels: implications for channel structure. *Ann. Rev. Biophys. Biophys. Chem.* 16:227–246.

Young, S. H., and J. W. Moore. 1981. Potassium ion currents in the crayfish giant axon. Dynamic characteristics. *Biophys. J.* 36:723–733.

Zimmerberg, J., and V. A. Parsegian. 1986. Polymer inaccessible volume changes during opening and closing of a voltage-dependent ionic channel. *Nature (Lond.).* 323:36–39.

Zimmerberg, J., and M. Whitaker. 1985. Irreversible swelling of secretory granules during exocytosis caused by calcium. *Nature (Lond.).* 315:581–584.